water

MDPI

Article

Influence of Substrate Material on Flow in Freezing Water Droplets—An Experimental Study

Erik Fagerström *, Anna-Lena Ljung, Linn Karlsson and Henrik Lycksam

Division of Fluid and Experimental Mechanics, Luleå University of Technology, SE-97187 Luleå, Sweden; anna-lena.ljung@ltu.se (A.-L.L.); linn.karlsson@ltu.se (L.K.); henrik.lycksam@ltu.se (H.L.)
* Correspondence: erik.fagerstrom@ltu.se

Abstract: Freezing water droplets are a natural phenomenon that occurs regularly in the Arctic climate. It affects areas such as aircrafts, wind turbine blades and roads, where it can be a safety issue. To further scrutinize the freezing process, the main objective of this paper is to experimentally examine the influence of substrate material on the internal flow of a water droplet. The secondary goal is to reduce uncertainties in the freezing process by decreasing the randomness of the droplet size and form by introducing a groove in the substrate material. Copper, aluminium and steel was chosen due to their differences in thermal conductivities. Measurements were performed with Particle Image Velociometry (PIV) to be able to analyse the velocity field inside the droplet during the freezing process. During the investigation for the secondary goal, it could be seen that by introducing a groove in the substrate material, the contact radius could be controlled with a standard deviation of 0.85%. For the main objective, the velocity profile was investigated during different stages of the freezing process. Five points along the symmetry line of the droplet were compared and copper, which also has the highest thermal conductivity, showed the highest internal velocity. The difference between aluminium and steel was in their turn more difficult to distinguish, since the maximum velocity switched between the two materials along the symmetry line.

Keywords: freezing; internal flow; water droplet; Marangoni flow; PIV

Citation: Fagerström, E.; Ljung, A.-L.; Karlsson, L.; Lycksam, H. Influence of Substrate Material on Flow in Freezing Water Droplets—An Experimental Study. *Water* **2021**, *13*, 1628. https://doi.org/10.3390/w13121628

Academic Editor: Xiangyu Hu

Received: 15 April 2021
Accepted: 7 June 2021
Published: 9 June 2021

1. Introduction

In the Arctic climate, the freezing of water is a phenomenon that occurs regularly. When water turns into ice, it can introduce new dangers; for example, ice on airplane wings that changes the aerodynamics, build-up on wind power blades and also the more common slippery roads. In these examples, the surfaces are subjected to a build-up of ice either by water droplets or humid air freezing onto them.

The freezing process of a water droplet has been the topic of comprehensive research [1], specifically areas such as visual study of freezing [2–8], singular tip [9–13], impact onto a surface [14–19] and tri-junction condition [20]. The research has concluded some important factors that affect the freezing process. Hao et al. [21] studied small, micro and micro/nano sized surface structures and compared them with smooth surfaces. Yue et al. [22] used four different surfaces, three with micro structures and one smooth. Both studies concluded that the roughness of the surface affects the freezing delay. De Ruiter et al. [23] studied the spreading of droplets. Sun et al. [24] used three substrate materials (copper, stainless steel and plexiglass) with varying thermal properties. The study showed that a difference exists in the freezing time for a supercooled droplet, although the droplets froze in a few milliseconds. Similarly, Stiti et al. [25] showed that, for a room temperature droplet, the freezing time varied for substrate materials with different thermal properties. Furthermore, Huang et al. [26] investigated how the contact angle relates to the freezing time, and concluded that a larger contact angle would have a longer freezing time. This shows that the shape of the water droplet, the material and the structure of the substrate surface are important when examining a freezing water droplet.

Another phenomenon that occurs inside the water droplet which has not been included in the previous studies is the internal flow. The phenomenon was first visualized by Kawanami et al. [27], who concluded that driving forces that have an influence on the internal flow are temperature gradients, buoyancy forces and surface tension resulting in the Marangoni convection. The internal flow of a water droplet was further numerically studied by Karlsson et al. [28,29]. They investigated the buoyancy forces and internal natural convection. In the numerical analysis, the Marangoni effect was not included, but they showed that the buoyancy force and the internal natural convection were important for the internal flow. Furthermore, Karlsson et al. [30] experimentally showed that there is a turn in the internal flow of a freezing water droplet. A probable cause for this is that the Marangoni effect generates a flow along the surface and up the middle of the droplet in the beginning of the freezing process. Then, after a few seconds, the natural convection becomes the dominating force and reverses the direction. In Karlsson et al. [31], internal flow in both freezing and evaporating droplets was compared and a shift in direction could be observed for both freezing and evaporating droplets. The setup in Karlsson et al. [30,31] required a transparent substrate for the laser as well as a thin layer of frost to initiate freezing. In particular, the need to generate a new layer of frost for each case induces an increased possibility of randomness regarding e.g., contact radius and height.

This paper investigates three areas experimentally; the first step is to reduce uncertainties and randomness in the freezing process by exchanging the frost layer with a mechanically constructed groove on the substrate to control the contact radius and to make the freezing process start immediately after impact; secondly, to modify the set up in Karlsson et al. [30,31], to enable opaque substrate materials; and, thirdly, to expand the knowledge of what affects the internal flow by studying how materials of substrates such as copper, aluminium and steel affect the internal flow in a freezing droplet.

2. Materials and Methods

In this section the experimental setup is described together with the experimental procedure and methods for uncertainty analysis.

2.1. Experimental Setup

Water droplets are released onto a metal plate with a diameter of 50 mm and a height of 2 mm. Three different substrate materials are investigated in this paper: copper, aluminium and steel. They are chosen due to their diverse conductivity as presented in Table 1. The plates have a circular groove that is 1 mm deep; it has an inner radius of 0.8 mm and an outer radius of 1.685 mm, see Figure 1. The groove's outer radius was calculated from a half-spherical droplet with a volume of 10 µL, i.e., aiming for a contact angle of 90° after the droplet had impacted on the surface.

Table 1. The thermal conductivity at 300 K for the three substrate materials. The conductivity of ice at 269 K is also included for [32].

Material	Thermal Conductivity [W m^{-1} K^{-1}]
Copper	400
Aluminium	238
Steel	45
Ice	2.1

Droplets with size 10 µL were used in the study. The droplets consist of deionized (DI) water seeded with fluorescent particles (microparticles GmbH PS-FluoRed) that has a diameter of 3.16 µm. The groove was filled up with 5.5 ± 0.1 µL DI water to get an ice layer that was approximately 1 mm. In Figure 1, the groove with an ice layer can be seen. Using the groove in this way is expected to increase the repeatability of the experiments with droplets being contained by the outer radius. Controlling the contact surface will then result in a contact radius and height that is very similar between different runs. The plate

was resting on an aluminium holder on-top of the Peltier element, which were cooled with a mixture of water and ice. The plate were enclosed by a plexiglass chamber to protect the droplet from forced convection. Four holes was made in the plexiglass chamber. One hole was made on the back of the chamber for the camera and one was created to the right to let the laser sheet pass through the droplet at a perpendicular angle to the camera. A third hole was needed on the top front corner for the hygrometer and lastly a hole was made on the top of the chamber to keep the pipette right above the center of the groove. The droplets were released by a pipette of model Finnpipette F1 10 µL that was kept in place by an optical rail. A thermocouple type K model 6206000 were used to record the temperature at the top of the plate. The experimental setup can be viewed in Figure 2.

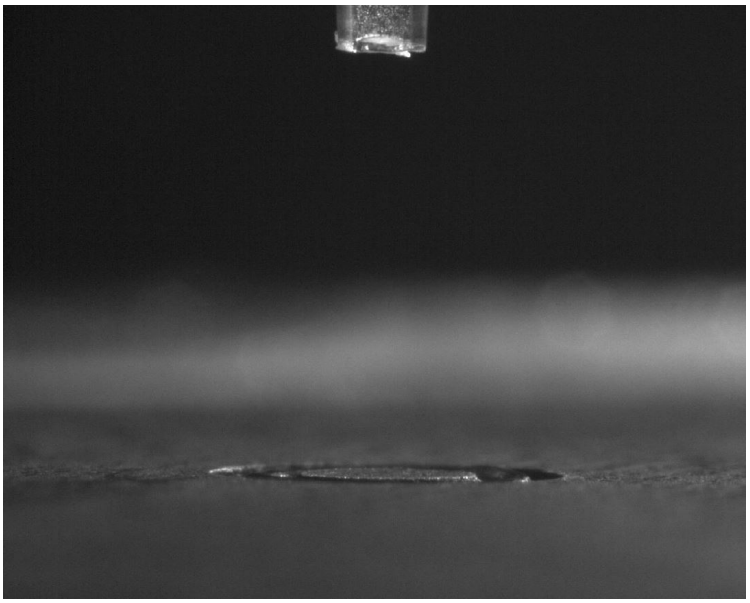

Figure 1. The groove with ice in it.

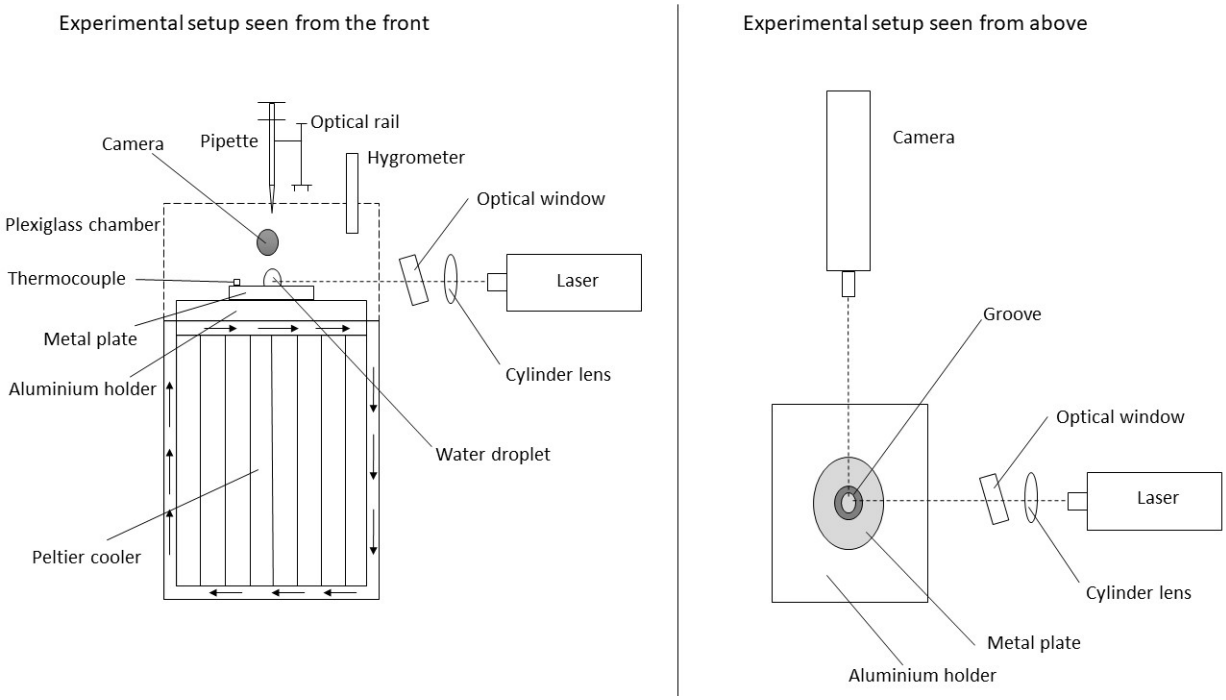

Figure 2. Schematic of the experimental setup.

The set up is similar to the experimental setup presented by Karlsson et al. [30,31] with the modification that the laser is now directed from the side instead of below. This was done so that the plates were not limited to transparent materials. A deficiency with this is that, due to the water/air boundary refracting the laser light, a small portion of the droplet edge furthest from the laser is darker in the images.

2.2. Experiment Procedure

- Fill the groove with DI water.
- Turn on the Peltier element to start the cooling of the plate.
- Remove the chamber and wipe the surface from all natural frost that has been formed from the moisture content of the air.
- Fill the pipette with the mix of DI water and particles and lower it into the chamber.
- Turn on the laser and start filming.
- Wait until the plate is at -8 °C.
- Release the droplet.
- When the singular tip can be observed and it is completely frozen, stop filming, turn off the laser and turn off the cooling of the plate.
- Wait until the droplets have melted and wipe all water off the plate and repeat.

2.3. Data and Uncertainty Analysis

Two things were required for the data analysis: the vector field inside the droplet and the boundary of the droplet. To find the vector field inside the droplet, the PIVlab package in Matlab was used. The images were analysed by defining the droplets boundary and then using the PIV algorithm FFT with three passes, pass 1 64 $\times$ 64, pass 2 32 $\times$ 32 and pass 3 16 $\times$ 16. The vectors were then revised by removing the ones located outside the boundary and lastly the vectors were calibrated by knowing the time between the frames and the diameter of the droplets base (i.e., that is the outer diameter of the groove). To find the boundary of the droplet, image analysis was performed in Matlab. First, the darker background pixels were removed with a threshold, and then a square was marked and image analysis was used to find the boundary. A known problem with images of water is that the water/air boundary will refract the light so that the particles will be distorted. Kang et al. [33] with corrections by Minor et al. [34] derived a correction mapping method to handle this issue. Using the method proposed by Kang et al. [33] and used by Karlsson et al. [30,31], the velocity field from PIVlab can be implemented with the boundary found from the image analysis. Then, the last step is to remove the vectors found in the ice. This is done by visually marking out the edge of the ice and correlating it to the vectors and removing them. After the procedure, the velocity vectors have been mapped to the correct place inside the droplet. The outer part of the droplet close to the edge can not be restored so some information is lost.

All experiments come with some uncertainty i.e., systematic errors and random errors. Some examples of systematic errors are that the droplet is not released exactly the same each time due to human error, the ratio of seeded particles is slightly off or not mixed well and in PIVlab calibrating a distance to a pixel could be slightly wrong. Random errors can be how the droplet is attached in the groove, vibrations causing the camera to move slightly, increasing/decreasing the pixel movement in the analysis and the amount of ice in the groove possibly varying a little, leading to a difference in contact angle and freezing time. An estimation of the errors for the mean velocity can be found using a repeatability test proposed by Coleman and Steele [35]. To reduce the errors and uncertainties to a minimum, the initial contact radius and height were determined from 81 experiments in total, and these are divided evenly with 27 experiments for each substrate material when studying the mean velocity. The experiments were performed following the predetermined procedure, performed over a few days and different batches of DI water seeded with particles were used to get rid of small variations. In the computer analysis, the radius, height and ice level are marked by hand so the analysis was performed five times to be able to get an average.

3. Results and Discussion

In the Results and Discussion section, three areas will be presented. First, repeatability of the droplet shape and size is discussed and compared with previous results where the droplets are released on a layer of frost [30,31]. Specifically, it is investigated how a predefined groove in the substrate affects the droplet contact radius, contact angle and height of the droplet—hence ensuring similar initial parameters (i.e., contact radius and height) for all experiments at the initiation of freezing. Secondly, the correlation between freezing time and contact angle is investigated and compared to results found in literature to ensure valid results. Thirdly, the influence of substrate material on the internal flow is investigated.

3.1. Droplet Radius and Contact Angle

To investigate the repeatability of the experiment, a study of the contact radius was performed for 81 experiments. An experiment was deemed valid if the ice level in the groove was at or below the top of the plate, if the droplet did not get stuck to the inner radius, and if there was movement in the droplet. Due to the manufacturing process of the plates, the outer radius for the three substrate materials became slightly different. Copper had a diameter of 3.364 mm, aluminium 3.471 mm and steel 3.610 mm. For the analysis, the radius was normalized by taking the measured droplet radius along the surface and dividing it by the radius of the groove. The experiments generated a mean normalized radius of 1.0085, which is 0.85% larger than the mean radius. For comparison, Karlsson et al. [30] obtained a contact radius of 1.677 mm with a standard deviation of $\pm$0.272 (16.19% of the mean) when a layer of natural frost was used to initiate freezing. This shows that the new method with a groove filled with ice could be used to generate uniform droplets for analysis. With this, the results would have a higher degree of certainty due to more similar settings regarding shape and size in the experiments. The ice layer initiated the freezing process instantly and were thus a good substitute compared to generating a layer of natural frost.

Looking at the mean radius individually for the three plates, there is some variation, and the mean normalized radius of copper, aluminium and steel are 1.0248, 1.0075 and 0.9931, respectively. The correlation between contact radius and contact angle is displayed in Figure 3a. The groove's outer radius was chosen so that it would generate a 90° contact angle for a 10 microliter droplet assuming a spherical shape. Copper had a radius closest to the calculated one with 1.682 mm instead of 1.685 mm, while aluminium and steel had 1.7355 mm and 1.805 mm, respectively. This means that the height would be notably smaller for aluminium and steel. From Figure 3b, it can be observed that the mean normalized height for copper, aluminium and steel are 1.0000, 0.9489 and 0.9192, respectively. In the same order of copper, aluminium and steel, the mean contact angle for the three substrate materials are 88.61°, 86.56° and 85.63°. The contact angle was calculated by

$$\theta = 2 \cdot arctan\left(\frac{h}{r}\right) \quad (1)$$

where h is the normalized height and r is the normalized radius. Comparing all 81 experiments, show a mean contact angle of 86.93° with a standard deviation of $\pm$3.347° (3.85% of the mean).

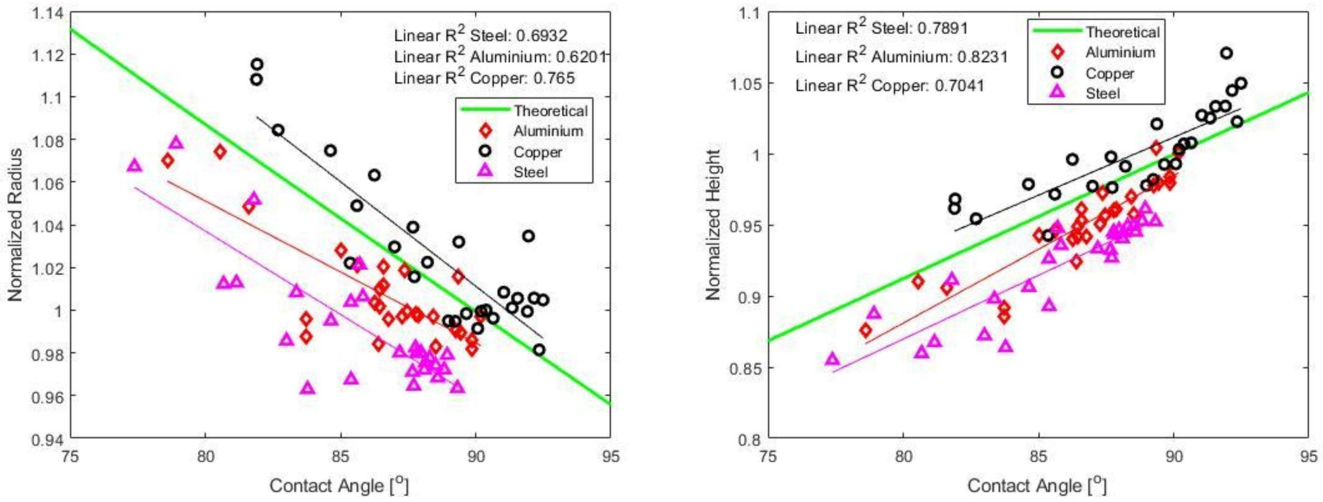

(a) Correlation between radius and contact angle.

(b) Correlation between height and contact angle.

Figure 3. Droplet radius and height as a function of contact angle. (**a**) shows the normalized radius as a function of the contact angle. (**b**) shows the normalized height as a function of a contact angle.

It was assumed that there would only be heat transfer at the cylinder in the middle of the groove, since the thermal conductivity is higher for metal than for ice as seen in Table 1. With a mean normalized radius of 1.0085, it can be assumed that the assumption holds, and that all droplets have the same surface area for heat transfer.

3.2. Freezing Time

As observed in Figure 4, the average freezing time is similar for the three substrates. Copper, aluminium and steel show average freezing time of 22.01 s, 21.52 s, and 22.47 s, respectively. This is in accordance with the results obtained by Sun et al. [24], where it was shown that the substrate material had only a small effect on the freezing time. The standard deviation in the same order, i.e., copper, aluminium and steel is 5.22%, 7.22% and 7.37%. The fastest individual freezing time, 18.58 s, was found for the aluminium plate while the maximum value was retrieved by the steel plate with a value of 25.67s. As observed in Figure 4a, the radius has no clear correlation with the freezing time, possibly due to the fact that the inner contact area between water and metal is approximately the same. As studied by Huang et al. [26], the freezing time is dependent on the contact angle. The contact angle retrieved in this study, showed a mean of 88.61°, 86.56° and 85.63° for copper, aluminium and steel, respectively. A linear correlation can be seen between the height and freezing time, see Figure 4b. As the contact radius between the metal and the droplet is controlled and the height somewhat varies, so does the freezing time, and then it follows that the freezing time is increased with a contact angle as mentioned by Huang et al. [26]. The results of the freezing time correlates with previous works showing that addition of a groove does not alter the behaviour, and the study thus continues with investigations of the internal flow.

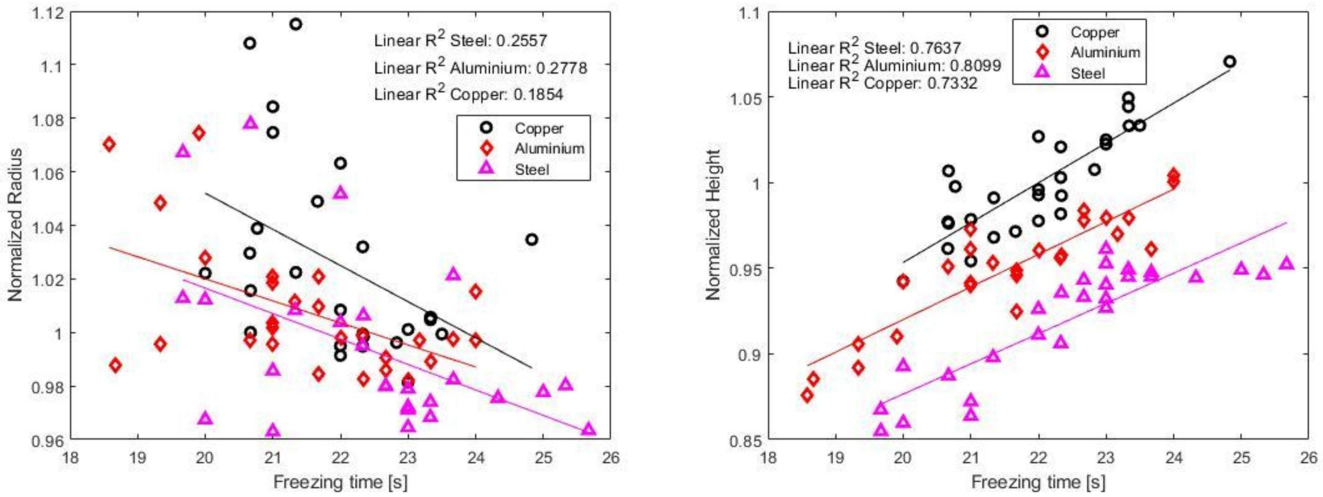

(a) Correlation between radius and freezing time.

(b) Correlation between height and freezing time.

Figure 4. Droplet radius and height as a function of freezing time. (**a**) shows the normalized radius as a function of freezing time. (**b**) shows the normalized height as a function freezing time.

3.3. Velocity Profile

To compare the velocity profiles for the different substrate materials, 27 experiments are analysed for each material to retrieve an average absolute velocity. The flow is investigated at two points in time throughout the freezing process. They are denoted as pre turn and after turn; pre turn is 0.75 s after the droplet has landed and started to freeze. The after turn is 0.25 s after the flow has changed direction of the internal flow, a bit into the freezing process. A specified time stamp was chosen instead of a scaled time due to the variation in freezing time for the same radius as seen in Figure 4a. The time it took for the flow to change direction varied and a suitable scaled time could therefore not be found. On average, the internal flow changed direction after 18.15% of the total freezing time with a max of 22.08% and a min of 8.57% of the freezing time. For the pre turn phase at 0.75 s, the internal flow had stabilized from the impact. In the after turn phase, the flow had enough time to change direction fully and the particles gained some velocity after the directional change.

In Figure 5a, the velocity profiles for the internal flow in the droplets are presented with dashed lines representing the flow after turn and the full lines representing the flow before the turn. The absolute velocity was studied at five different points along the symmetry line. It was chosen to use five points in the analysis to replicate the analysis method provided in Karlsson et al. [30], where a similar setup was used. The camera is set at a slight angle so the ice front is seen as a disc, see Figure 5c. This could mean that the data point at the ice boarder could in fact be the velocity of the freezing front and not the internal flow. Figure 5c also shows where the five data points are located in relation to the vector field.

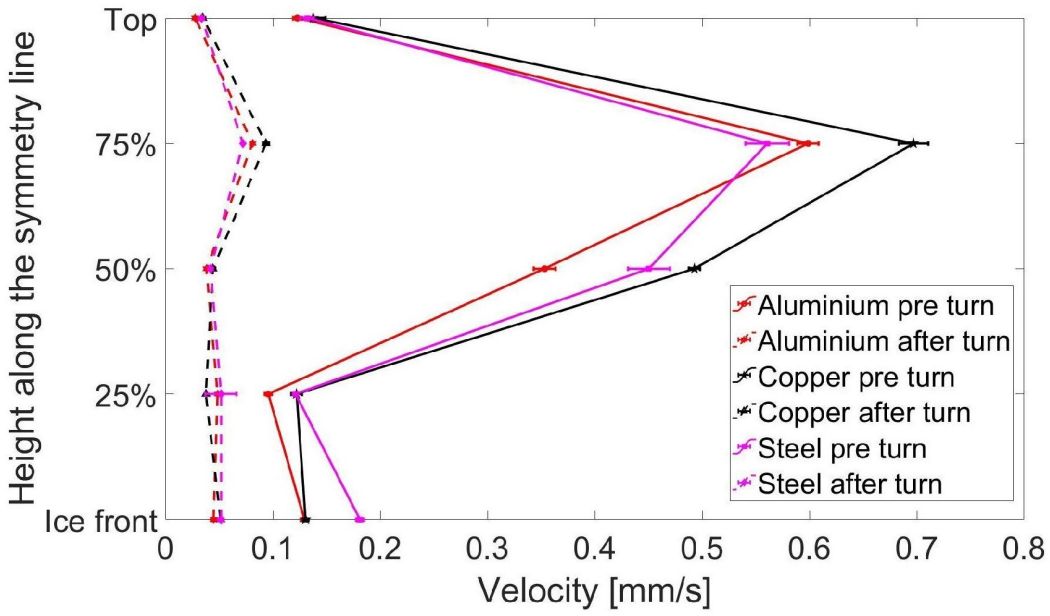

(a) Velocity profile along the symmetry line.

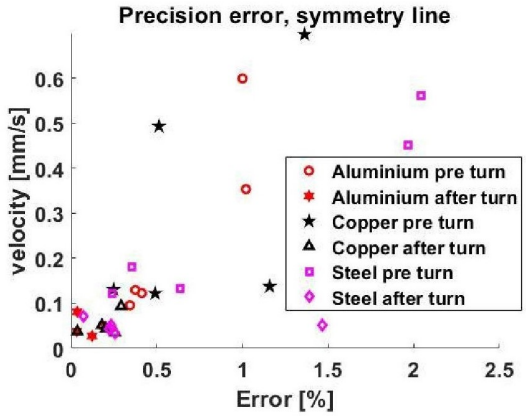

(b) The precision error along the symmetry line.

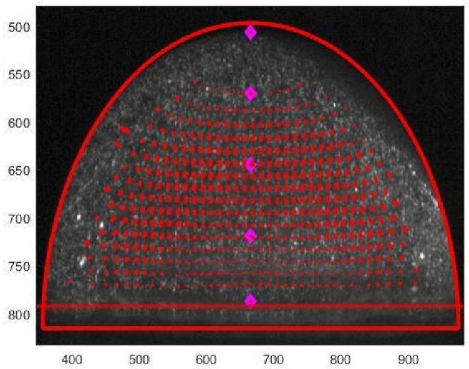

(c) The five data points where the velocity were taken from before correction.

Figure 5. In (**a**), the velocity profile for the different substrate materials can be seen throughout the droplet for pre and after turn. In (**b**), the precision error can be seen for all the points in (**a**). In (**c**), the velocity field after application of the correction method proposed by Kang et al. [33] is displayed together with the five data points

Comparing the velocity profiles in Figure 5a shows that copper has the highest velocity, while the differences between aluminium and steel are more difficult to quantify. Looking at the highest velocity at 75% of the droplets' height, the velocities are in the order of copper, aluminium and steel. This follows the same order as thermal conductivity, with copper having the highest. It should, however, be pointed out that this behavior is not observed for all measurement points when comparing steel and aluminium. This phenomenon is displayed both before and after the directional change in the velocity. The results are additionally analysed with the repeatability test proposed by Coleman and Steele [35]. Looking at the precision error for all the points in Figure 5b and quantified in Table 2, it can be seen that the highest error is 2.0409% for steel, which is considered sufficient for the purpose of this study. For copper, the highest error is 1.3627% and for aluminium 1.0202%.

Table 2. Precision error at the symmetry line for the five data points as presented in Figure 5b.

Pre Turn	Copper [%]	Aluminium [%]	Steel [%]	After Turn	Copper [%]	Aluminium [%]	Steel [%]
Top	1.1586	0.4123	0.6355	Top	0.2568	0.1215	0.2567
75%	1.3627	0.9999	2.0409	75%	0.2917	0.0351	0.0706
50%	0.4127	1.0202	1.9674	50%	0.2026	0.0327	0.2223
25%	0.4905	0.3430	0.2403	25%	0.0358	0.1969	1.4643
Ice front	0.2478	0.3743	0.3556	Ice front	0.1785	0.2288	0.2339

4. Conclusions

The experimental work show details about the internal flow in a freezing droplet both quantitatively and qualitatively. Parameters such as contact radius and height of the droplet, as well as freezing time, are also obtained. With the experimental set-up presented in this paper, it is also possible to use opaque substrate materials, in addition to transparent substrate that was required in the previous works [30,31].

- From the experiments it can be concluded that the contact radius and angle of a droplets impact on a substrate can be controlled to a higher degree when using a groove filled with ice rather than impinging on a flat surface covered with a layer of natural frost. The repeatability study of 81 experiments showed to a rather high degree that, when introducing a groove in the plate, the contact radius could be predetermined with a standard deviation of 0.85%.
- The experimental results show that the freezing time is dependent on the contact angle and hence also the height of the droplet. A higher contact angle will increase the time of freezing. Dependence on contact radius is not as visible in this work since the contact radius between metal and droplet is rather constant due to the groove.
- The velocity profile was determined inside the droplet before and after the direction change for the three substrate materials. At the point where the velocity was highest (75% between the top and freezing front), copper had the highest velocity, followed by aluminium and then steel. The internal velocities thus follows the thermal conductivites with copper having the highest thermal conductivity and steel the lowest. This order only applies for the fastest point; both at the top and at a height of 50%, steel had a higher velocity than aluminium. The overall velocity difference between aluminium and steel is, however, rather small. Copper is 16.39% faster than aluminium, and aluminium is 5.78% faster than steel at the highest velocity. There is thus a difference in internal flow between the substrates, but the difference between aluminium and steel is not as distinct as for copper.

Author Contributions: Conceptualization, E.F., A.-L.L. and L.K.; methodology, E.F., L.K. and H.L.; software, E.F.; validation, E.F. and A.-L.L.; formal analysis, E.F. and A.-L.L.; investigation, E.F.; resources, A.-L.L.; data curation, E.F.; writing—original draft preparation, E.F.; writing—review and editing, E.F., A.-L.L., L.K. and H.L.; visualization, E.F.; supervision, A.-L.L.; project administration, E.F.; funding acquisition, A.-L.L. All authors have read and agreed to the published version of the manuscript.

Funding: This research received no external funding.

Institutional Review Board Statement: Not applicable.

Informed Consent Statement: Not applicable.

Data Availability Statement: Data sharing not applicable.

Conflicts of Interest: The authors declare no conflict of interest.

References

1. Mengjie, S.; Chaobin, D.; Tomohira, H.; Eiji, H. Review of experimental data associated with the solidification characteristics of water droplets on a cold plate surface at the early frosting stage. *Energy Build.* **2020**, *223*, 110103.
2. Liu, Z.; Zhang, X.; Wang, H.; Meng, S.; Cheng, S. Influences of surface hydrophilicity on frost formation on a vertical cold plate under natural convection conditions. *Exp. Therm. Fluid Sci.* **2007**, *31*, 789–794. [CrossRef]
3. Jin, Z.; Dong, Q.; Jin, S.; Yang, Z. Visualization of the freezing and melting process of a small water droplet on a cold surface. In Proceedings of the International Conference on Fluid Dynamics and Thermodynamics Technologies (FDTT 2012), Singapore, 17–18 March 2012; Volume 33.
4. Jung, S.; Tiwari, M.K.; Doan, N.V.; Poulikakos, D. Mechanism of supercooled droplet freezing on surfaces. *Nat. Commun.* **2012**, *3*, 1–8. [CrossRef] [PubMed]
5. Jin, Z.; Jin, S.; Yang, Z. Visualization of icing process of a water droplet impinging onto a frozen cold plate under free and forced convection. *J. Vis.* **2013**, *16*, 13–17. [CrossRef]
6. Schremb, M.; Tropea, C. Solidification of supercooled water in the vicinity of a solid wall. *Phys. Rev. E* **2016**, *94*, 052804. [CrossRef]
7. Zhang, X.; Wu, X.; Min, J. Freezing and melting of a sessile water droplet on a horizontal cold plate. *Exp. Therm. Fluid Sci.* **2017**, *88*, 1–7. [CrossRef]
8. Yao, Y.; Yang, R.; Li, C.; Tao, Z.; Zhang, H. Investigation of the freezing process of water droplets based on average and local initial ice fraction. *Exp. Heat Transf.* **2020**, *33*, 197–209. [CrossRef]
9. Wang, J.; Liu, Z.; Gou, Y.; Zhang, X.; Cheng, S. Deformation of freezing water droplets on a cold copper surface. *Sci. China Ser. E Technol. Sci.* **2006**, *49*, 590–600. [CrossRef]
10. Enríquez, O.R.; Marín, Á.G.; Winkels, K.G.; Snoeijer, J.H. Freezing singularities in water drops. *Phys. Fluids* **2012**, *24*, 091102. [CrossRef]
11. Marin, A.G.; Enriquez, O.R.; Brunet, P.; Colinet, P.; Snoeijer, J.H. Universality of tip singularity formation in freezing water drops. *Phys. Rev. Lett.* **2014**, *113*, 054301. [CrossRef]
12. Schetnikov, A.; Matiunin, V.; Chernov, V. Conical shape of frozen water droplets. *Am. J. Phys.* **2015**, *83*, 36–38. [CrossRef]
13. Ismail, M.F.; Waghmare, P.R. Universality in freezing of an asymmetric drop. *Appl. Phys. Lett.* **2016**, *109*, 234105. [CrossRef]
14. Jin, Z.; Zhang, H.; Yang, Z. Experimental investigation of the impact and freezing processes of a water droplet on an ice surface. *Int. J. Heat Mass Transf.* **2017**, *109*, 716–724. [CrossRef]
15. Jin, Z.; Zhang, H.; Yang, Z. The impact and freezing processes of a water droplet on different cold cylindrical surfaces. *Int. J. Heat Mass Transf.* **2017**, *113*, 318–323. [CrossRef]
16. Ju, J.; Jin, Z.; Zhang, H.; Yang, Z.; Zhang, J. The impact and freezing processes of a water droplet on different cold spherical surfaces. *Exp. Therm. Fluid Sci.* **2018**, *96*, 430–440. [CrossRef]
17. Yao, Y.; Li, C.; Tao, Z.; Yang, R.; Zhang, H. Experimental and numerical study on the impact and freezing process of a water droplet on a cold surface. *Appl. Therm. Eng.* **2018**, *137*, 83–92. [CrossRef]
18. Wang, L.; Kong, W.; Wang, F.; Liu, H. Effect of nucleation time on freezing morphology and type of a water droplet impacting onto cold substrate. *Int. J. Heat Mass Transf.* **2019**, *130*, 831–842. [CrossRef]
19. Zhang, X.; Liu, X.; Wu, X.; Min, J. Impacting-freezing dynamics of a supercooled water droplet on a cold surface: Rebound and adhesion. *Int. J. Heat Mass Transf.* **2020**, *158*, 119997. [CrossRef]
20. Schultz, W.; Worster, M.; Anderson, D. Solidifying sessile water droplets. In *Interactive Dynamics of Convection and Solidification*; Springer: Berlin/Heidelberg, Germany, 2001; pp. 209–226.
21. Hao, P.; Lv, C.; Zhang, X. Freezing of sessile water droplets on surfaces with various roughness and wettability. *Appl. Phys. Lett.* **2014**, *104*, 161609. [CrossRef]
22. Yue, X.; Liu, W.; Wang, Y. Freezing and melting of sessile droplet on micro-and hierarchically-structured silicon surfaces. *Appl. Therm. Eng.* **2019**, *161*, 114185. [CrossRef]
23. De Ruiter, R.; Colinet, P.; Brunet, P.; Snoeijer, J.H.; Gelderblom, H. Contact line arrest in solidifying spreading drops. *Phys. Rev. Fluids* **2017**, *2*, 043602. [CrossRef]
24. Sun, M.; Kong, W.; Wang, F.; Liu, H. Impact freezing modes of supercooled droplets determined by both nucleation and icing evolution. *Int. J. Heat Mass Transf.* **2019**, *142*, 118431. [CrossRef]
25. Stiti, M.; Castanet, G.; Labergue, A.; Lemoine, F. Icing of a droplet deposited onto a subcooled surface. *Int. J. Heat Mass Transf.* **2020**, *159*, 120116. [CrossRef]
26. Huang, L.; Liu, Z.; Liu, Y.; Gou, Y.; Wang, L. Effect of contact angle on water droplet freezing process on a cold flat surface. *Exp. Therm. Fluid Sci.* **2012**, *40*, 74–80. [CrossRef]
27. Kawanami, T.; Yamada, M.; Fukusako, S.; Kawai, H. Solidification characteristics of a droplet on a horizontal cooled wall. *Heat Transf.-Jpn. Res. Co-Spons. Soc. Chem. Eng. Jpn. Heat Transf. Div. ASME* **1997**, *26*, 469–483. [CrossRef]
28. Karlsson, L.; Ljung, A.L.; Lundstrom, S. Influence of internal natural convection on water droplets freezing on cold surfaces. In Proceedings of the CONV-14: International Symposium on Convective Heat and Mass Transfer, Kusadasi, Turkey, 8–13 June 2014; Begel House Inc.: Danbury, CT, USA, 2014.
29. Karlsson, L.; Ljung, A.L.; Lundström, T.S. Modelling the dynamics of the flow within freezing water droplets. *Heat Mass Transf.* **2018**, *54*, 3761–3769. [CrossRef]

30. Karlsson, L.; Lycksam, H.; Ljung, A.L.; Gren, P.; Lundström, T.S. Experimental study of the internal flow in freezing water droplets on a cold surface. *Exp. Fluids* **2019**, *60*, 1–10. [CrossRef]
31. Karlsson, L.; Ljung, A.L.; Lundström, T.S. Comparing Internal Flow in Freezing and Evaporating Water Droplets Using PIV. *Water* **2020**, *12*, 1489. [CrossRef]
32. Nordling, C.; Österman, J. *Physics Handbook for Science and Engineering*; Studentlitteratur AB: Lund, Sweden, 2006.
33. Kang, K.H.; Lee, S.J.; Lee, C.M.; Kang, I.S. Quantitative visualization of flow inside an evaporating droplet using the ray tracing method. *Meas. Sci. Technol.* **2004**, *15*, 1104. [CrossRef]
34. Minor, G.; Oshkai, P.; Djilali, N. Optical distortion correction for liquid droplet visualization using the ray tracing method: Further considerations. *Meas. Sci. Technol.* **2007**, *18*, L23. [CrossRef]
35. Coleman, H.; Steele, W. *Experimentation, Validation, and Uncertainty Analysis for Engineers*; John Wiley & Sons, Inc.: Hoboken, NJ, USA, 2009.